

**Title :** Improvement of aeroelastic instability of shallow  $\pi$  section

**Authors:** Yoshinobu Kubo, Kenji Sadashima, Eiki Yamaguchi, Kusuo Kato

**Affiliation:** Kyushu Institute of Technology, Kitakyushu, Japan

**Author:** Yuzo Okamoto

**Affiliation:** Shin-nippon Steel Company, Tokyo, Japan

**Author:** Takashi Koga

**Affiliation:** Sumitomo Heavy Industry, Tokyo, Japan

**Abstract:** From economical point of view, a two-plate-girder bridge section has been examined as a bridge section for a long span suspension bridge. The two-plate-girder bridge section of H or  $\pi$  section inherently has not good aerodynamic performances, as shown by the accident of the Tacoma Narrows Bridge with H section type bridge girder. On the contrary, in the present paper, it is tried to find the possibility of the aerodynamic performance improvement of the two-plate-girder bridge section of the  $\pi$  section by changing the intervals between the two plate girders. Referring to wind tunnel test results, in the vortex-excited vibration in heaving vibration mode, the on-set wind velocity and the vibration amplitude decrease with interval between two plate girders, and the flutter on-set wind velocity increases. These results show the possibility of aerodynamic performance improvement of the two-plate-girder bridge section.

**Keywords:** long span suspension bridge, two-plate-girder bridge section, aerodynamic performances

**Main Text:**

## 1. INTRODUCTION

H and  $\pi$  sections are the two-plate-girder sections that sufficiently satisfy the structural requirement. H section is easy to vibrate under wind action as shown in the collapse of the Tacoma Narrows Bridge. Therefore there is no idea to use the H section for the long span bridge girder section. Although the  $\pi$  section in Fig.1 is also easy to vibrate under wind action when the two plate girders are placed near the ends of the floor, the  $\pi$  section is regarded as one of bridge girder sections satisfying the cost performance of a long span suspension bridge. Because the  $\pi$  section is a simple structure for the bridge girder as well as the H section, the two plate girders are movable within satisfying structural requirement and the movement of the plate girders enables to change flow pattern around the bridge section to suppress the vibration under wind action by using an idea of mutual interaction of separation flow (Y. Kubo, 1993). According to the idea, can be controlled the reattachment of separation flow from leading edge of the floor by changing the location of the plate girders, thus the bridge section becomes aerodynamically stable.

The present paper deals the aerodynamic performance of the  $\pi$  sections with various locations of two plate girders and aims to examine the usefulness of the idea of mutual interaction of separation flow for control of the aerodynamic vibration of the  $\pi$  section. If the idea is useful, the design of the bridge section

can be done from viewpoint of fusing the structural design and the aerodynamic design. Up to now, the shape of bridge girder section of almost long span bridges has been determined through the aerodynamic examination after the structural design was completed. It is the problem in the design of bridge girder that the structural and the aerodynamic approaches are separated. The shape of the bridge girder should be determined by fusing both structural and aerodynamic design processes. If the aerodynamic instability is improved by only changing the position or the shape of the structural members, without using non-structural members of fairings or flaps so on, the cost for the bridge must be considerably reduced.

## 2. WIND TUNNEL TESTS

Wind tunnel tests were conducted in a closed circuit wind tunnel with test section of 0.9x1.8m. 2-degree of freedom vibration system was used to examine the aerodynamic performances of the bridge girder section with two plate girders as shown in Fig.1. The side length ratio of the model section was  $B/D = 10$ . The parameter  $C$  was varied from 0.5  $D$  to 2.0  $D$  by changing the location of the plate girders. For measuring 3 components of aerodynamic forces (lift, drag, aerodynamic moment), was used a 3-component aerodynamic force balance. Flow visualization was also conducted by smoke wire method to understand the behavior of reattachment of separation flow from leading edge of the bridge section.

The wind tunnel test conditions were followings. The mass of the model was 50.23 kg/m and moment of inertia of mass was 0.0657 kg m<sup>2</sup>/m. Natural frequency for heaving and torsional vibrations were 2.17Hz and 4.19Hz, respectively. The logarithmic structural damping for heaving and torsional vibrations was 0.0048 and 0.0013.

## 3. EXPERIMENTAL RESULTS

### 3.1 Aerodynamic responses of $\pi$ section

Fig.2 shows the experimental results of aerodynamic responses in heaving vibrations. With the increase in overhanging parameter  $C$ , decreases the on-set wind velocity of vortex-excited vibration and the amplitude of the vibration. Referring to the reported experimental results for rectangular prisms, Strouhal number of the rectangular prisms takes the smaller value for the larger side length ratio. In the present case, assuming that apparent ratio of side length is defined by ratio of interval between plate girders to the bridge girder height, the case with larger value of  $C$  corresponds to the case with smaller side length ratio of rectangular prism. Considering the correspondence with the rectangular prism, the case with larger Strouhal number corresponds to the case with lower on-set wind velocity of the vortex-excited vibration. According to the experimental results in Fig. 2, occurs the vortex-excited vibration at lower wind velocity for larger  $C$ . Assuming that the ratio of interval to height of two plate girders corresponds to the side length ratio of a rectangular prism, the ratio of the present case is equal to  $B/D = 6$  to 9. In the rectangular prism,  $B$  is the length along stream direction and  $D$  is the length normal to stream direction. Fig.3 shows plots of on-set wind velocity of the vortex-excited vibration in heaving vibration mode against  $C/D$ . The

on-set wind velocity decreases linearly with the parameter  $C$ . Since Strouhal number is equal to a reciprocal number of on-set wind velocity expressed in reduced wind velocity, Strouhal number is estimated with 0.059 for  $C/D = 0.5$  and 0.143 for  $C/D = 2.0$  from Fig.3. Strouhal number, however, is 0.186 and 0.203 for rectangular prisms with  $B/D = 6$  and 9, respectively (Y. Nakamura, 1991). These values do not correspond to the estimated values. Therefore, another approach is needed to make clear the relationship between on-set wind velocity and  $C/D$ .

Figs. 4 and 5 show aerodynamic responses of torsional vibration of the  $\pi$  section girder with various values of  $C/D$ . The plots shown as “excited” in the figures are responses observed in the free vibration condition after the model was compulsorily vibrated. According to these figures, when the parameter  $C$  is less than  $1.5D$ , the on-set wind velocity in torsional mode increases with  $C$ . The on-set wind velocity of flutter  $V_r (= 27, 45, 73, 88)$  is proportional to the ratio  $C/D (= 0.5, 0.75, 1.0, 1.25)$  as shown in Fig.6. On the other hand, in the cases of  $C/D$  larger than 1.5, the flutter was not induced as shown in Fig.5.

Referring to the experimental results for aerodynamic vibration, the aerodynamic performance was remarkably improved by putting two girders in inner portion of the bridge deck. In the cases of  $C/D$  larger than 1.5, only the vortex-excited vibrations were observed and the amplitude decreased with  $C/D$ , as shown in Fig. 5. As the mechanism for improving the aerodynamic performances, is considered the interaction effect of separation flow from the leading edge with that from the tip of the upstream plate girder. The detail of the mechanism is following. When the separation flow from the leading edge of the bridge deck flows down, the separation flow collides with the web of the upstream plate girder and main separation flow is induced from the tip of the upstream plate girder as shown in Fig.7. The separation bubble on the upper side of the floor becomes smaller with increase of  $C/D$  and the separation bubble behaves as well as the separation bubble on surfaces of a shallower section. As a result, the flutter on-set wind velocity increases with  $C/D$ . The detail will be discussed in a following chapter.

### 3.2 Aerodynamic forces of $\pi$ section

Figs. 8 to 10 show measured results of aerodynamic forces (drag and lift forces and aerodynamic moment) to angle of attack. Fig. 8 shows the relationship between drag force and angle of attack for various  $C/D$ . The drag force decreases with increase in  $C/D$  for overall angle of attack. The drag force coefficients of the  $\pi$  section for  $C/D = 0.5$  and 2.0 are 1.65 and 1.3, respectively. Therefore, the drag force of  $C/D = 2.0$  decreases by a quarter of  $C/D = 0.5$ . The maximum value of drag force appears at zero degrees of angle of attack and minimum value at 4 degrees of positive angle of attack. The drag force at 4 degrees is about 3 quarters of the value of zero degrees of angle of attack. It is concluded from these results that the drag force decreases when the plate girders are moved into inner portion in the floor system.

Fig. 9 shows lift force coefficient to angle of attack. The lift force takes negative value in region of angle of attack less than 2 degrees. Since the negative lift force means downward force, the negative lift force induces tensile force in the hanger cable of suspension bridge and the stay cable of cable-stayed bridge under high wind velocity. It is equal to the increase of stiffness of the structure to introduce the tensile force into cables of cable structures. Therefore, the  $\pi$  section has an advantage of increasing the structural stiffness under wind action.

Fig. 10 shows coefficient of aerodynamic moment to angle of attack. By comparing aerodynamic moment with lift force, the point of application of the lift force can be estimated. When the lift force and the aerodynamic moment have the same sign, the lift force applies further than the center of the deck in the windward as shown in Fig. 11. In angle of attack larger than 4 degrees, since the lift force is positive and the aerodynamic moment is positive, the lift force applies further than the center of the deck in the windward. In cases of  $C/D = 0.5$  and  $1.0$ , the lift force is negative and the aerodynamic moment is positive in angle of attack less than around 2 degrees. Then the lift force applies further than the center of deck in the leeward. When angle of attack moves from  $+8$  to  $-8$  degrees, outlines on the movement of the point of application of the lift force for  $C/D = 0.5$  are considered as that the lift force applies at near center when angle of attack is 8 degrees, at further point than the center in the windward for 4 degrees and at further point in the leeward for negative angle. At angle of attack  $-8$  degrees, the lift force applies at center of deck again. In case of  $C/D = 2.0$ , the point of application of lift force moves from the windward to the leeward and moves again to the windward.

Judging from the above-mentioned results, it can be concluded that moving the plate girders into inner portion is equal to making the bridge section more streamline like shape.

### *3.3 Aerodynamic response of $\pi$ section with wall type crash barrier*

Another experiments were conducted by using the model with  $C/D = 2.0$ , which had the best aerodynamic performance among the cases experimented in the present study. The experiment was conducted to investigate the influence of a wall type crash barrier to the aerodynamic performance of the  $\pi$  section. The arrangement of crash barrier is shown in Fig.12.  $\theta$  is the angle composed by floor level and connecting line between floor tip and crash barrier tip. The experiments were conducted under the conditions of  $\theta = 90, 60, 45, 30, 15$  degrees. Fig.13 shows the response results in torsional vibration for the crash barrier with  $\theta = 90$  degrees for various  $C/D$ . According to the results, even the case most stable in torsional vibration, it becomes remarkably unstable by adding the wall type crash barrier with  $\theta = 90$  degrees. In order to improve the aerodynamic instability shown in Fig. 13, the separation flow interference effect, which was developed by one of the authors (Y. Kubo, 1993), was applied. According to the previous research, when the angle  $\theta$  is 30 degrees, the aerodynamic stability is secured. Because the separation flow from the leading edge of the floor collides on the crash barrier web when  $\theta$  is larger than 30 degrees and the main separation flow is induced at the tip of the crash barrier and the bridge section becomes unstable. On the other hand, when  $\theta$  is around 30 degrees, passes the separation flow from leading edge of the floor through around the tip of the wall type crash barrier. And the separation flow controls the separation flow from the tip of the barrier to improve the aerodynamic instability of the bridge section. Fig. 14 shows the experimental results after the separation flow interference method was applied. In the cases except  $C/D = 2.0$ , the vortex-excited and the flutter are induced. Only the case of  $C/D = 2.0$  is stable. This result was obtained by using the method of separation flow mutual interference on both upper and lower sides of the bridge deck.

### *3.4 Flow visualization around $\pi$ section*

Flow visualization was conducted to understand the flow behavior around the bridge section. The model for flow visualization was elastically supported by cross leaf springs to vibrate in torsional mode.

Fig.15 shows the flow behavior of the  $\pi$  section with  $C/D = 0.5$  and  $2.0$ . The photos were taken in a moment when the  $\pi$  section moved in clockwise rotation from level position during torsional vibration. According to the figures, the size of separation bubble on upper side of the section with  $C/D = 0.5$  is bigger than that with  $C/D = 2.0$ . The shape of separation bubble for  $C/D = 0.5$  is also clearer than that for  $C/D = 2.0$ . The reattachment point for  $C/D = 0.5$  is further from leading edge than that for  $C/D = 2.0$ . Judging from the results, it can be considered that the thickness of the section at leading edge becomes thin with increase in  $C/D$  and the upper side separation bubble becomes smaller. Therefore, the case with  $C/D = 2.0$  is more approximate to the streamlined shape than the case with  $C/D = 0.5$ . On the lower side of the case with  $C/D = 0.5$ , starts the curl of the separation flow from the tip of the upstream plate girder at stage . On the other hand, does not curl the separation flow of the case with  $C/D = 2.0$ . The difference of flow behavior induces the difference in aerodynamic responses.

Fig. 16 shows the flow behavior of the  $\pi$  section with  $C/D = 2.0$  and crash barrier wall with  $\theta = 90$  and  $30$  degrees. The separation flow behavior on lower side is almost same regardless of  $\theta$ . The difference between two cases is the separation flow behavior on the upper side of the section. The separation flow of the case with  $\theta = 90$  degrees strongly curls from the tip of the upstream crash barrier wall on upper side of the section. On the other hand, in the case with  $\theta = 30$  degrees, attaches the separation flow from the leading edge of the floor to the tip of crash barrier wall and flows down without curling.

The flow visualization gives useful information to understand the improvement method of aerodynamic performance of the  $\pi$  section.

#### 4 CONCLUDING REMARKS

The present research started based on the fundamental concept to develop the economical bridge girder section that is satisfying social demands. One of the key points to accomplish the concept is to combine the structural design and the aerodynamic design. The present paper shows one example of the possibility to fuse the structural design and the aerodynamic design by choosing suitable arrangement of structural members. The following is concluding remarks associated with aerodynamic performances of the  $\pi$  section.

- 1) Even if the  $\pi$  section composed of two plate girders and floor, it is possible to achieve improvement of aerodynamic instability by not fairing or spoiler so on but only structural members.
- 2) The movement of plate girders to inner portion makes the  $\pi$  section approximate to streamlined shape and aerodynamically stable.
- 3) The separation flow interference method is useful to stabilize aerodynamic instability of bluff body like a bridge girder. The crash barrier wall is one of factors which makes the bridge deck aerodynamically unstable. By applying the separation flow interference method to the crash barrier wall, the bridge deck with wall type crash barrier becomes aerodynamically stable.
- 4) The flow visualization helps understandings about improvement of aerodynamic instability of the  $\pi$  section. In order to understand the mechanism of aerodynamic instability in detail, surface pressure

measurement should be conducted. Then, will be made clear the relationship between pressure distribution and overhanging ratio  $C/D$  and the relationship between pressure distribution and separation flow interference method.

## 5 *References*

Y. Kubo, K. Honda, K. Tasaki, K. Kato, 1993

Improvement of aerodynamic instability of cable-stayed bridge deck by separated flows mutual interference method,

Journal of Wind Engineering and Industrial Aerodynamics, Vol.49, pp.553-564.

Y. Nakamura, Y. Ohya, H. Tsuruta, 1991

Experiments on vortex shedding from flat plates with square leading and trailing edges,

Journal of Fluid Mechanics, Vol.222, pp.437-447.

Figures for the paper titled as "Improvement of aeroelastic instability of shallow  $\pi$  section", submitted for BBAA4.

By Yoshinobu Kubo

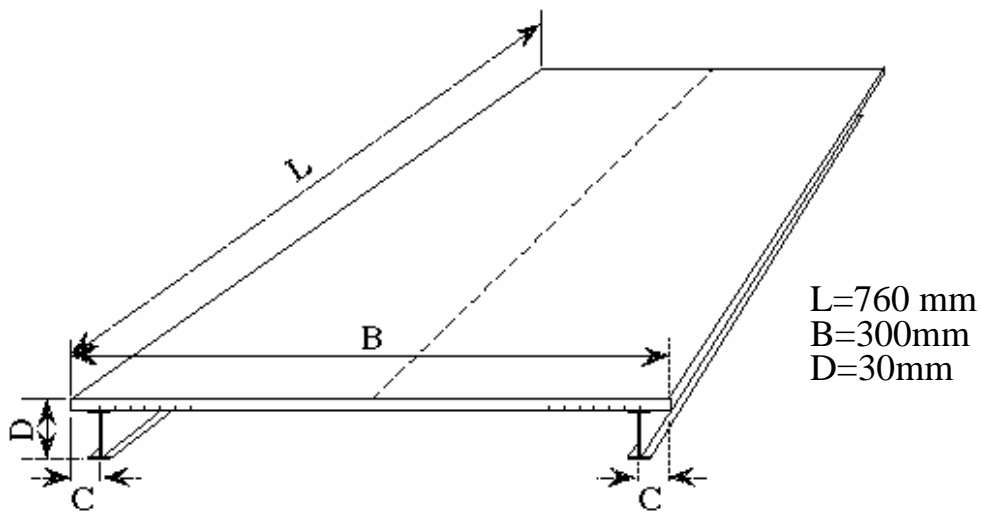


Fig.1 Model for wind tunnel tests of  $\pi$  section girder

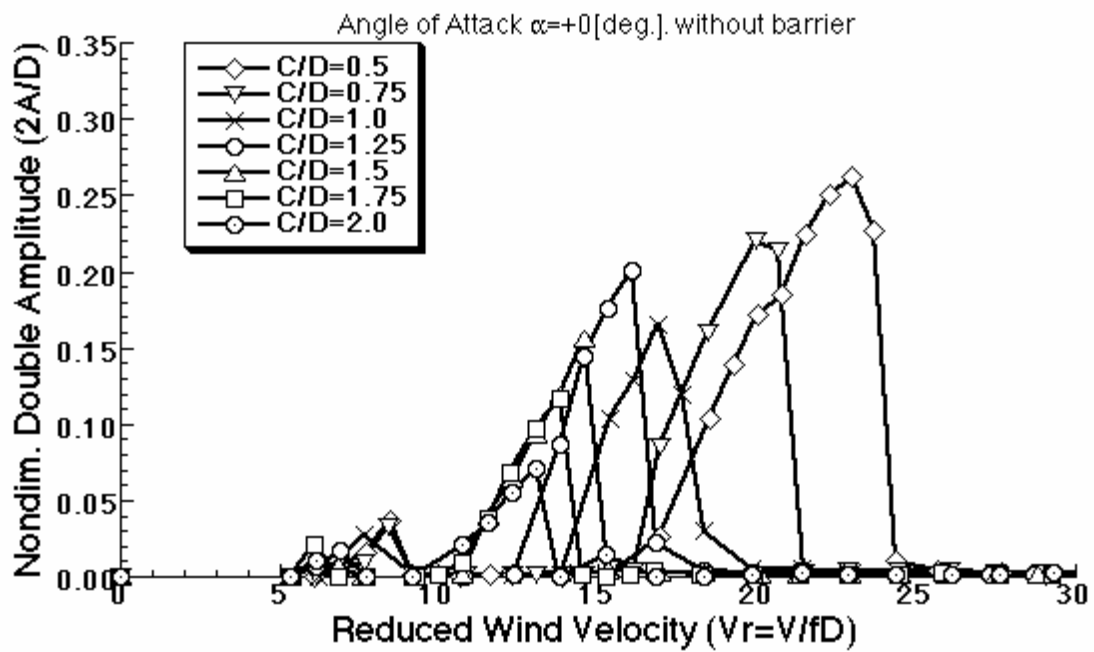


Fig.2 Aeroelastic response of heaving vibration mode ( $\alpha = 0$  deg.)

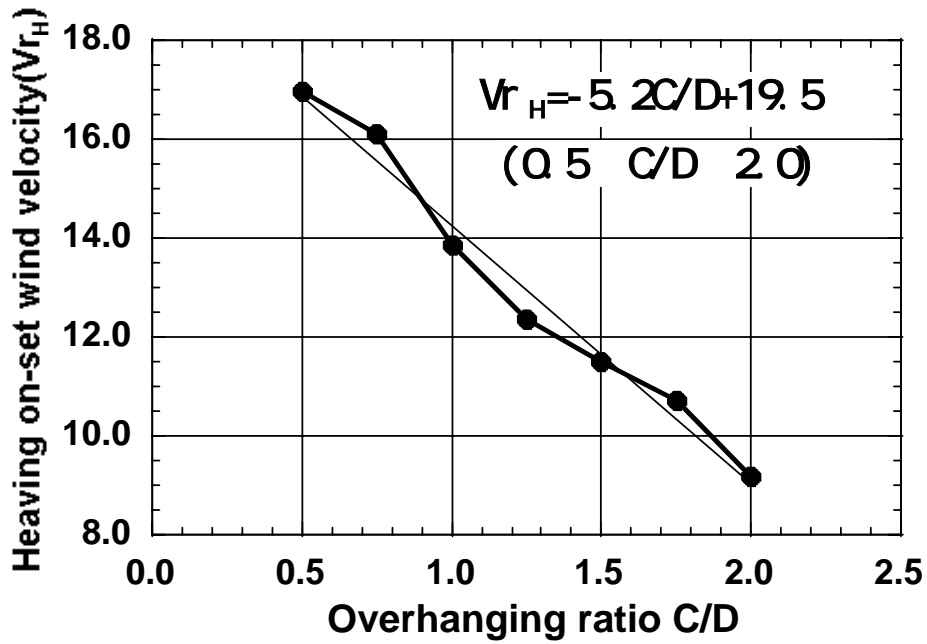


Fig. 3 Relationship between on-set wind velocity and C/D in heaving vibration mode

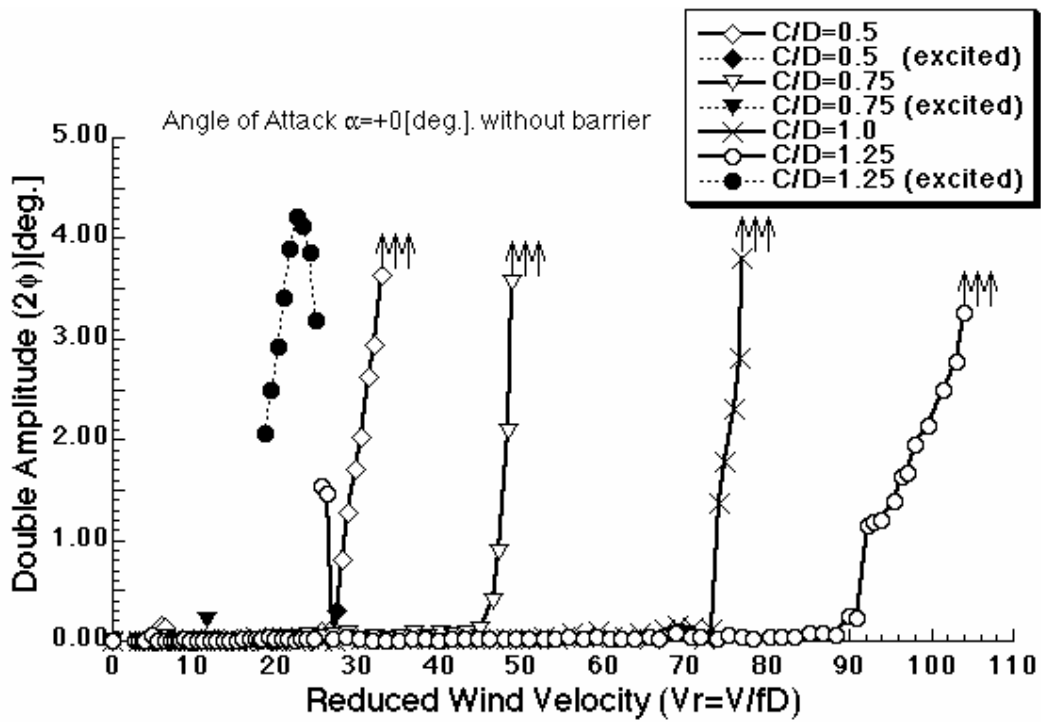


Fig.4 Torsional responses of  $\pi$  section girder with C/D = 0.5 to 1.25

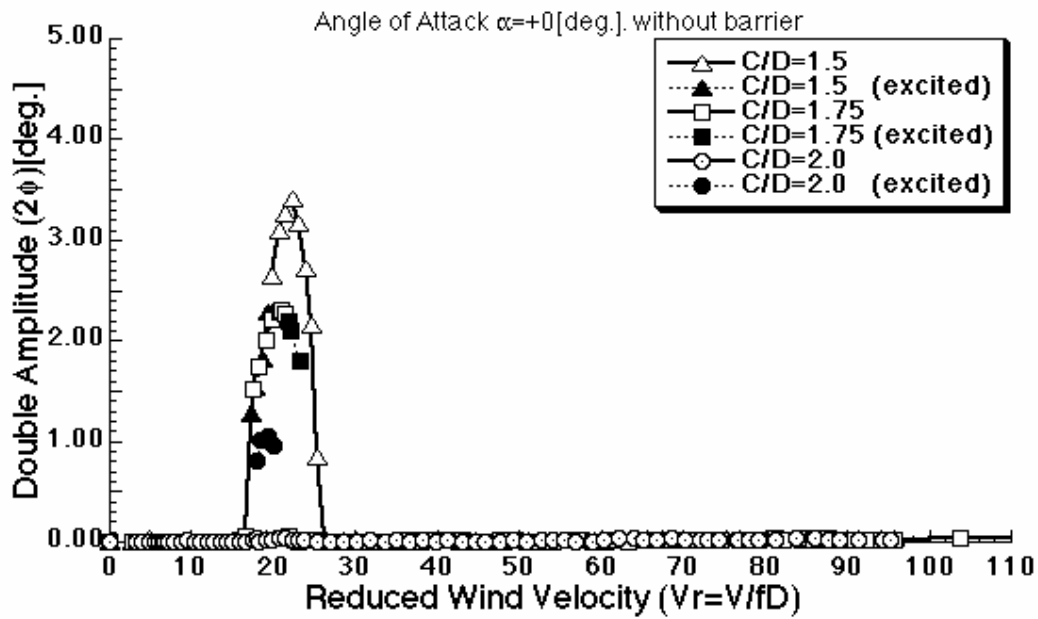


Fig.5 Torsional responses of  $\pi$  section girder with  $C/D = 1.5$  to  $2.0$

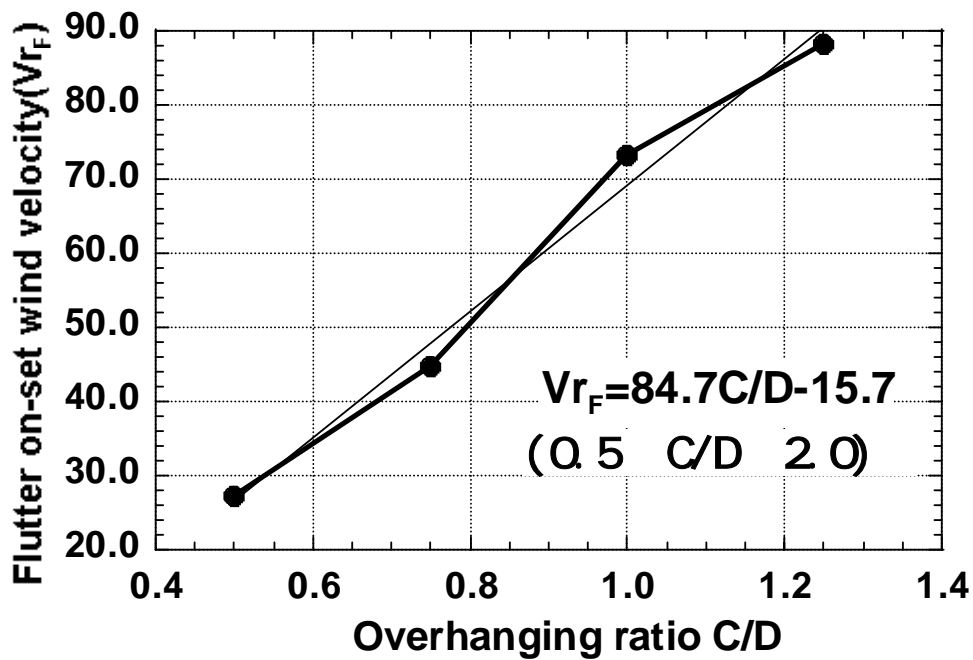


Fig. 6 Relationship between flutter on-set wind velocity and  $C/D$



Fig. 7 Estimated flow pattern based on  $C/D$

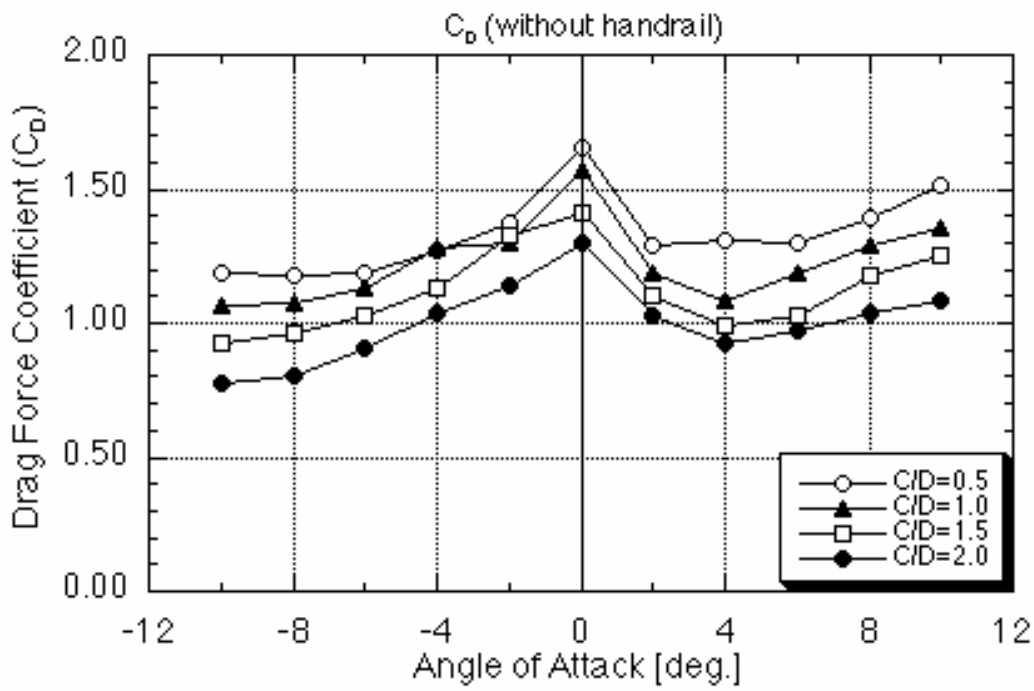


Fig. 8 Drag force coefficient of  $\pi$  section

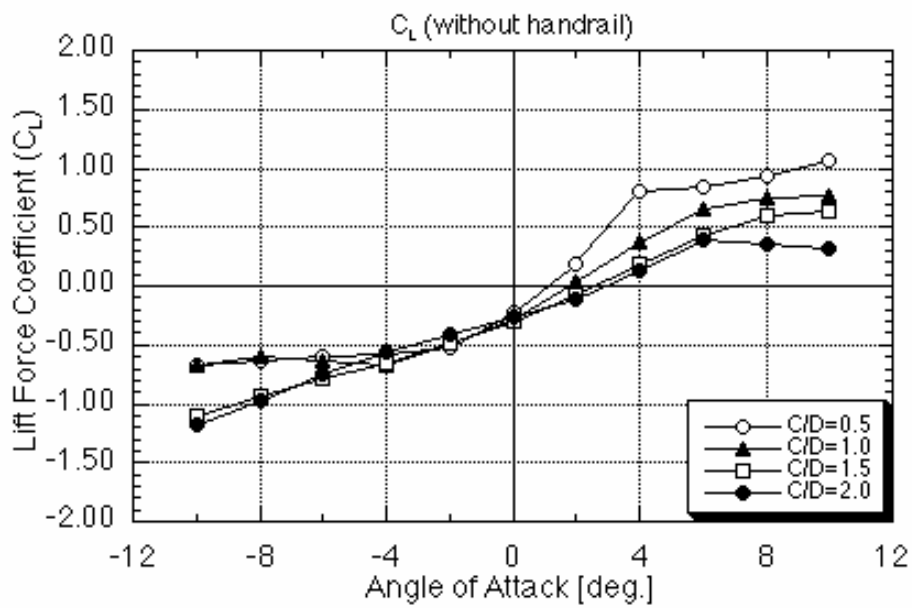


Fig. 9 Lift force coefficient of  $\pi$  section

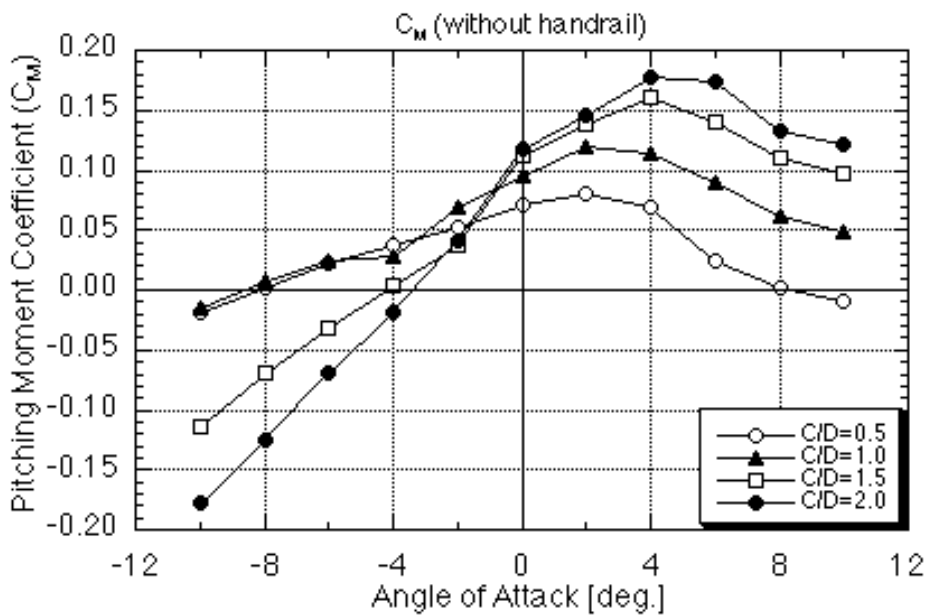


Fig. 10 Aerodynamic moment coefficient of  $\pi$  section

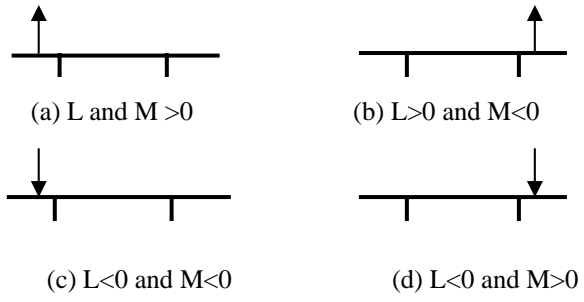


Fig. 11 Location and direction of lift force estimated from aerodynamic moment

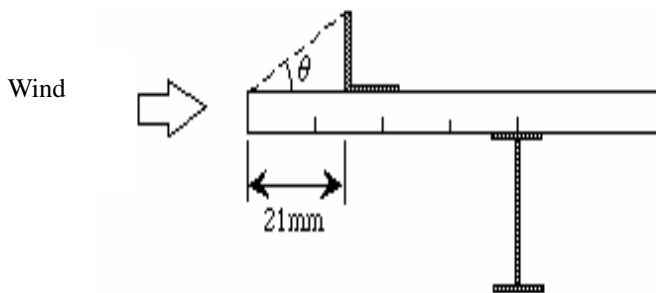


Fig.12 Location of wall type crash barrier

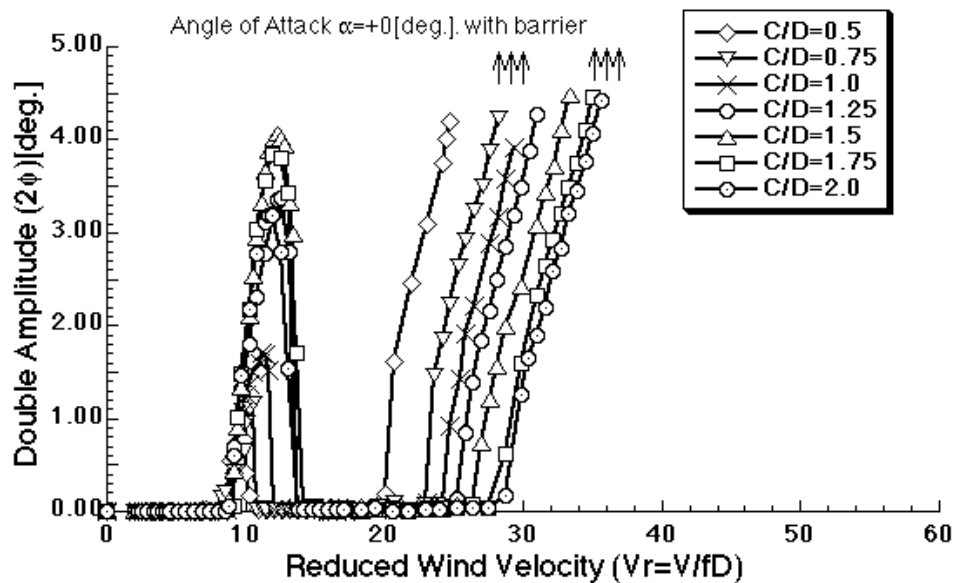


Fig. 13 Aerodynamic response in torsional vibration with wall type crash barrier with  $\theta = 90$  degrees

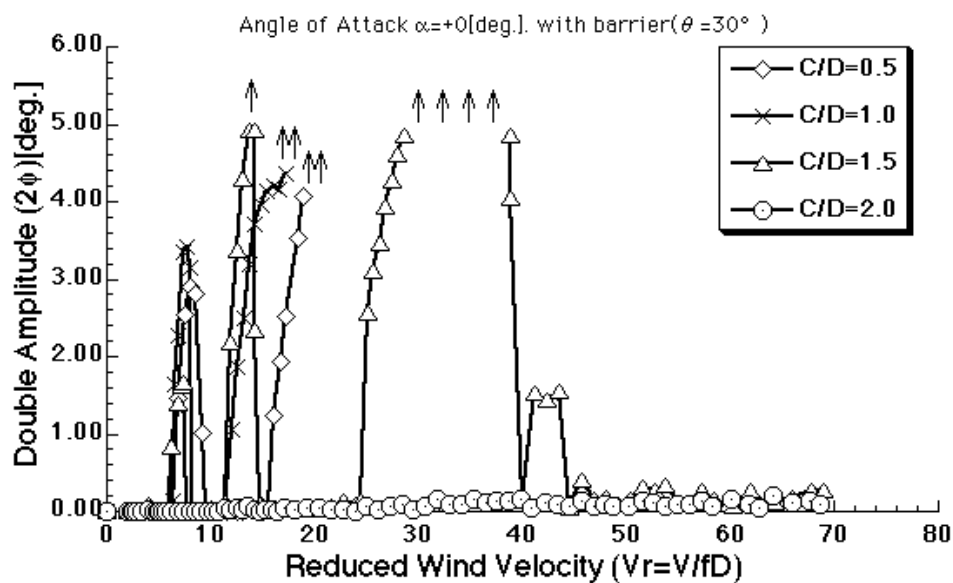
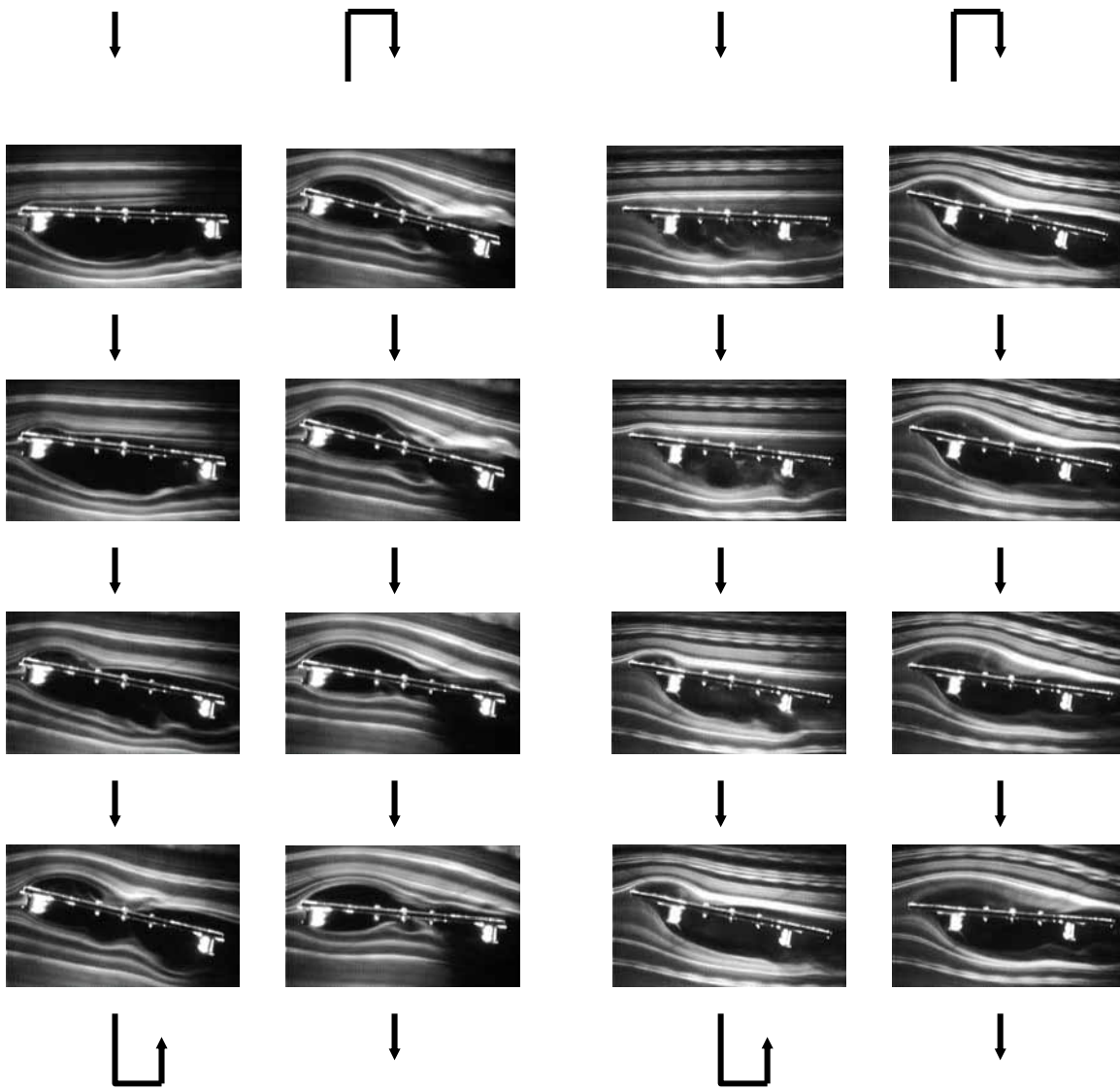


Fig. 14 Aerodynamic response in torsional vibration with wall type crash barrier with  $\theta = 30$  degrees



(a) with  $C/D=0.5$

(b) with  $C/D=2.0$

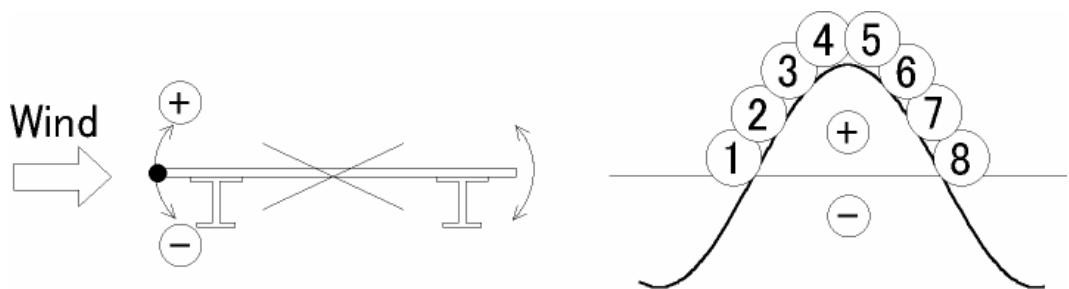


Fig. 15 Flow visualization of  $\pi$  section during torsional vibration

